Optomechanical Studies of Lithium Intercalation in Amorphous Molybdenum Thin Films

A. Gorenstein,*[a] A. Lourenço,[a] and J. Scarminio*[b]

[a]*DFA/IFGW/UNICAMP, CP 6165 CEP 13084-970, Campinas, SP, Brazil*
[b]*Departamento Física, UEL, CP 6001, CEP 86051-970, Londrina, PR, Brazil*

ABSTRACT

In this work, we studied radio-frequency reactively sputtered molybdenum oxide thin films. Thin films with distinct stoichiometries were obtained by varying the oxygen flow and maintaining all other deposition parameters constant. The relationship between optical, electrochemical, and mechanical behavior of the films submitted to lithium intercalation in an aprotic electrolyte is reported. Films deposited at low oxygen flow (B-films) are substoichiometric molybdenum oxide, with composition MoO_{3-x} ($0 < x < 1$). Films deposited at high oxygen flow (T-films) approach the MoO_3 stoichiometry. B-films have a greater concentration of optically active sites and a more open structure when compared to T-films.

Introduction

Different growth techniques are currently used for molybdenum oxide thin-film deposition[1] such as thermal evaporation,[2] sputtering,[3] chemical vapor deposition (CVD)[4], electrodeposition,[5] etc. The ability of these materials to exchange lithium ions reversibly with an electrolyte has been explored in microbatteries[6] and optical devices.[1] The as-grown films are either transparent or slightly blue and show a deep blue color upon lithium insertion. The electrochemical insertion reaction is

$$MoO_x + ye^- + yLi^+ \rightleftarrows Li_yMoO_x \qquad [1]$$

The thin-film electronic-band and crystallographic structure govern the kinetics of this reaction and the charge capacity of the material,[1] as well as the optical behavior of the system. Each deposition technique or deposition condition leads to films with distinct microstructure and stoichiometry. As a consequence, the ability of the material to accept lithium ions and its optical behavior upon lithium insertion vary. The relationship among all these parameters is far from clear, in part due to a lack of systematic work exploring different deposition parameters and insufficient physical and chemical characterization of the as-grown and intercalated films.

In this work, we studied RF reactively sputtered molybdenum oxide thin films. Thin films with distinct stoichiometries were obtained by varying the oxygen flow and maintaining all other deposition parameters constant. The objective of this work was to study the relationship between optical, electrochemical, and mechanical behavior of the films submitted to lithium intercalation in an aprotic electrolyte.

Experimental

Films were produced by RF reactive sputtering. Substrates were thick glass plates (Corning 7059, used in spectral transmittance measurements), flexible indium-tin oxide (ITO) covered thin glass plates (0.15 mm, used in stress measurements), or ITO-covered thick glass plates (used in *in situ* monochromatic transmittance measurements). Deposition conditions are shown in Table I. Table II presents the thicknesses of the films, as measured by profilometry (α-step profilometer, Tencor Instruments).

Spectral transmittance of films deposited onto thick glass was measured with a Lambda-9 Perkin-Elmer spectrophotometer.

Lithium intercalation was promoted by electrochemical means from a 0.1 *M* $LiClO_4$/propylene carbonate electrolyte. A lithium foil was used as the counterelectrode. The pseudo-reference electrode was metallic Ag (2.72 V *vs.* Li in this electrolyte). The electrodes were mounted in a sealed Teflon electrochemical cell with two parallel optical windows. All the preparation was done in a dry box, filled with Ar and with less than 1.0 ppm of water. Potentiodynamic and galvanostatic experiments were performed using a 273 EG&G potentiostat/galvanostat. Monochromatic transmittance (λ = 632.8 nm) and stress measurements were performed simultaneously with an experimental setup described elsewhere.[7] We considered the transmittance of cell and electrolyte as 100%. Stress changes are reported with samples in the oxidized state as our arbitrary reference.

Results

The molybdenum oxide films were deposited at seven different oxygen flow rates (ϕ) ranging from 1.5 to 8.0 sccm. All films were amorphous when observed by standard x-ray diffraction technique. The deposition rate (t) obtained from thickness measurements and deposition time is shown in Fig. 1. Initially, t increases with the increase of ϕ (region A, Fig. 1) but decreases for higher ϕ (region B, Fig. 1).

Figure 2 shows the transmittance as a function of wavelength for the as-grown films. The transmittance of the films deposited at low ϕ is shown in Fig. 2a. The film deposited at ϕ = 1.5 sccm is metal-like. Films deposited at ϕ = 1.65 and 1.75 sccm are deep blue. The transmittance of the films deposited at high ϕ is shown in Fig. 2b. The films deposited with ϕ in the range ϕ = 2 to 8 sccm are slightly blue (ϕ = 2.0 sccm) or transparent for all other flows.

The optical density change (OD) is obtained from transmittance measurements (T), using the relation $OD = -\log T$. The absorption coefficient α can be calculated by the relation[2]

$$\alpha = 2.303\ OD/d \qquad [2]$$

* Electrochemical Society Active Member.

Table I. Deposition conditions.

Equipment	Balzers BAE-250 deposition system
Target	Metallic molybdenum
Target/substrate distance	12 cm
RF power	100 W
Atmosphere	O_2-Ar
Initial pressure	1.5×10^{-6} mbar
Deposition pressure	7.0×10^{-3} mbar
O_2 flow	1.5 to 8 sccm

Table II. Sample thickness.

O_2 flow during deposition (sccm)	Thickness (nm)
1.5	200
1.65	200
1.75	200
2	200
3	165
5	140
8	120

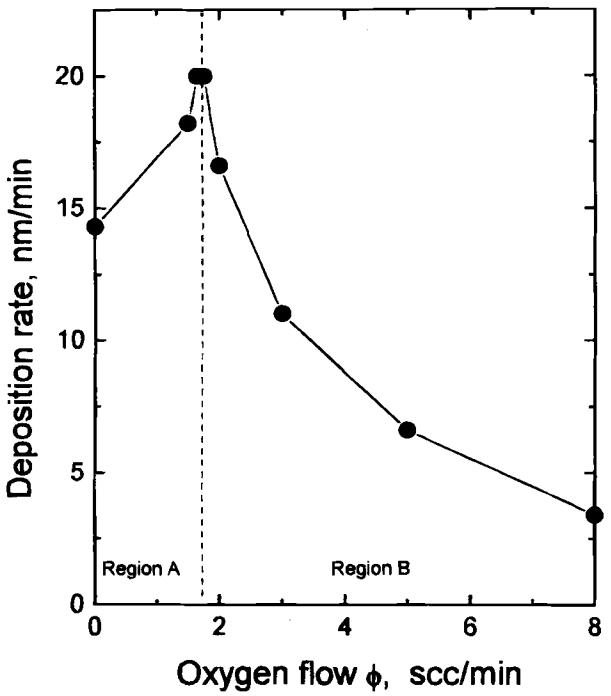

Fig. 1. Deposition rate as a function of oxygen flow during sample deposition.

where d is the thickness of the film. In the high absorption region, the absorption coefficient α obeys the well-known relationship[8]

$$\alpha h\nu = B\,(h\nu - E_{opt})^n \qquad [3]$$

where $h\nu$ is the photon energy, B is a constant, E_{opt} is the optical gap of the material, and the index n can assume different values depending on the type of electronic transition. The value $n = 2$ indicates absorption by nondirect transitions. The optical properties of many amorphous thin oxide films follow relation 3 with $n = 2$. Values of E_{opt} can be obtained from the linear region of a $(\alpha h\nu)^{1/2}$ *vs.* $h\nu$ plot, by extrapolation toward zero absorption. This procedure was used in the present work, and the values of E_{opt} as a function of oxygen flow are shown in Fig, 3. It can be seen in this figure that the optical gap increases with an increase in ϕ. Values of optical bandgap for the present films are in the range 2.8 eV for low ϕ to 3.2 eV at high ϕ.

In what follows, the blue films deposited at low oxygen flows are called B-films, and the transparent films deposited at high oxygen flows are called T-films.

Lithium intercalation in the MoO_x films was investigated, as described in the Experimental section. The cell was assembled in a dry box, and the initial open-circuit potential (E_r) before intercalation was measured. Figure 4 shows the results. The span in E_r is 0.3 V. B-films have an E_r more positive than the values measured for the T-films. The range of electroactivity on potentiodynamic cycling is also displaced for the different films, as is shown below.

Figure 5a shows the j/E curve, obtained in potentiodynamic conditions, for a B-film (solid curve) and a T-film (dashed curve). Figures 5b and c show the simultaneously

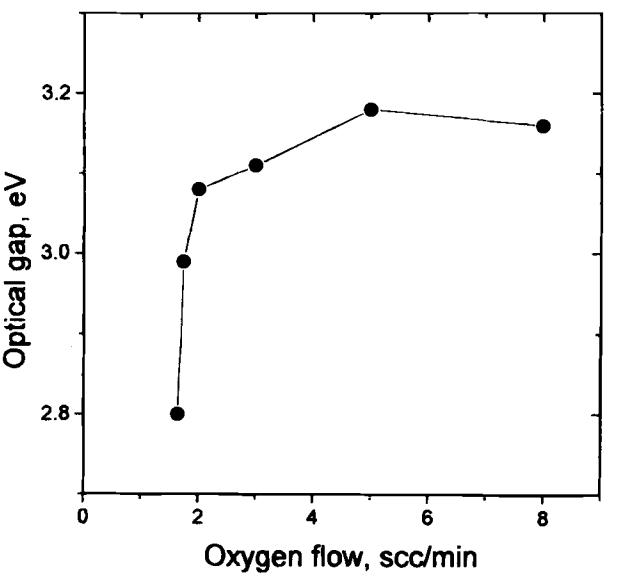

Fig. 3. Optical gap as a function of oxygen flow during deposition (see text).

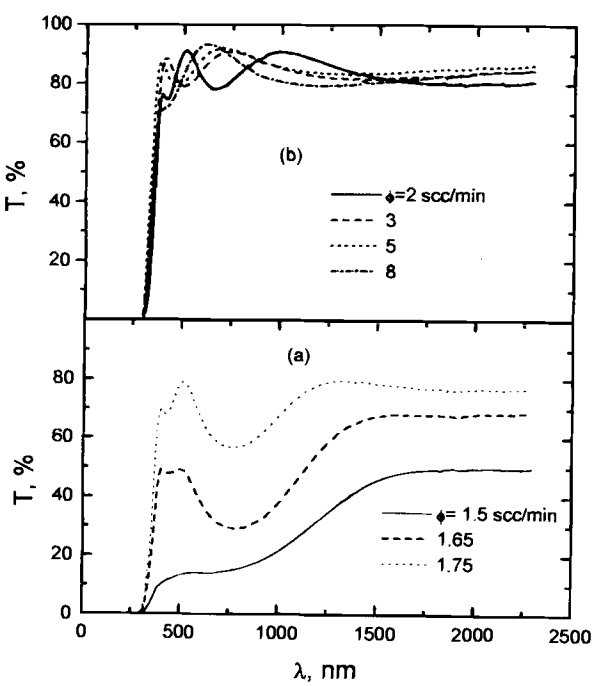

Fig. 2. Transmittance as a function of wavelength, for as-grown samples deposited onto 7059 glass plates.

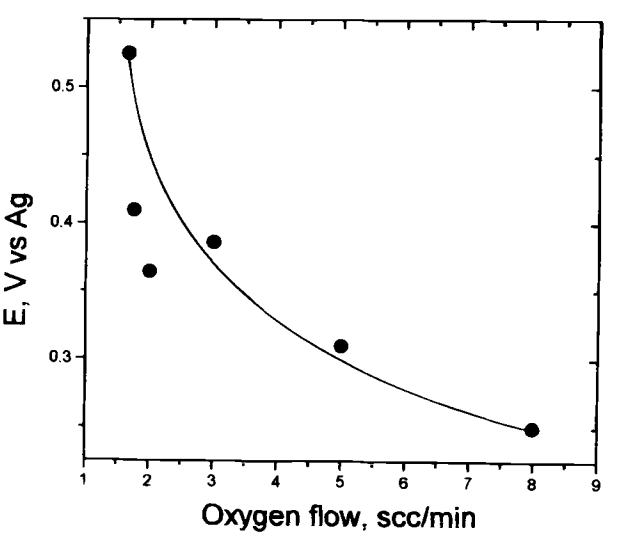

Fig. 4. Initial rest potential as a function of oxygen flow during deposition.

measured optical density change (ΔOD, at λ = 632.8 nm) and the associated charge change (ΔQ), respectively. The onset of the cathodic current is at 0.6 V for the B-film and 0 V for the T-film (Fig. 5a). For the B-film, ΔOD is 0.25 for an inserted charge of 12 mC/cm^2. This last value corresponds to an inserted charge per unit volume of 6×10^5 mC/cm^3. In this experiment, ΔOD is not a linear function of the inserted or extracted charge, as can be seen in Fig. 6a. The coloration efficiency (defined as $\Delta OD/\Delta Q$) is 40 cm^2/C at the beginning of the intercalation reaction and falls to 16 cm^2/C after approximately 2.5 mC/cm^2 of intercalated lithium. In the anodic cycle, the coloration efficiency is constant and has a value of -20 cm^2/C for the B-film. ΔOD for the T-film is much lower than the value observed for B-films (Fig. 5b), even if more cathodic potentials are attained at this scan rate. For the T-film, ΔOD is 0.04 for an inserted charge of 4 mC/cm^2 (inserted charge per unit volume of 3.3×10^5 mC/cm^3). The initial coloration efficiency is 19 cm^2/C and falls to 8 cm^2/C after 1.5 mC/cm^2 of intercalated lithium (Fig. 6b). The coloration efficiency is constant in the cathodic cycle and has a value of -15 cm^2/C, for the T-film. It can be seen from Fig. 5b and c that the intercalation process is fully reversible for the B-films since both the ΔOD and ΔQ are closed curves. The T-film presented some irreversibility at the conditions of this experiment. However, if the potential is held at the extreme anodic potential value for some time, the optical density returns to the initial value, and all inserted charge is extracted.

Figure 7a shows the j/E curve, also obtained in potentiodynamic conditions, and Fig. 7b and c show the simultaneously measured stress change ($\Delta\sigma$) and the associated charge change (ΔQ), respectively. Typical results for B-films and T-films are shown in this figure. The scan was reversed at a higher cathodic limit in comparison with the results presented in Fig. 5. The onset of the cathodic current is at 0.5 V for the B-film and at O V for the T-film (Fig. 7a). Figure 7b shows an increase in the compressive stress during the cathodic reaction, for both films. This increase in compressive stress is associated with an increase of the thin film global volume. The reverse process is observed in the anodic cycle (Fig. 7b). For the B-film, $\Delta\sigma$ attains the value 350×10^6 N m^2 (350 MPa), for an insertion charge of 23 mC/cm^2. The stress change per unit charge $\Delta\sigma/\Delta Q$ is not constant on cycling (Fig. 8a). The initial value is $\Delta\sigma/\Delta Q$ = 9 MPa mC^{-1}. This value increases to 18 MPa mC^{-1} after approximately 3.5 mC/cm^2 of intercalated lithium. In the anodic cycle, $\Delta\sigma/\Delta Q$ has the constant value $\Delta\sigma/\Delta Q = -40$ MPa mC^{-1}. The stress developed by the T-film is $\Delta\sigma$ = 210 MPa, for an insertion charge of 13 mC/cm^2. The initial value of $\Delta\sigma/\Delta Q$ is 19 MPa mC^{-1}, increasing slightly to 22 MPa mC^{-1} after 2.5 mC/cm^2 of intercalated lithium (Fig. 8b). In the anodic cycle, $\Delta\sigma/\Delta Q$ is also constant for the T-film, and has the value $\Delta\sigma/\Delta Q = -26$ MPa mC^{-1}. Also, neither the $\Delta\sigma$ *vs.* E curve nor the ΔQ *vs.* E curve is a closed figure at these deeper charge intercalation levels (Fig. 7b and c). It has to be pointed out that the B-films used in the experiments described in Fig. 7 present a reversible behavior if the scan is performed with the same cathodic potential limit of the experiments described in Fig. 5.

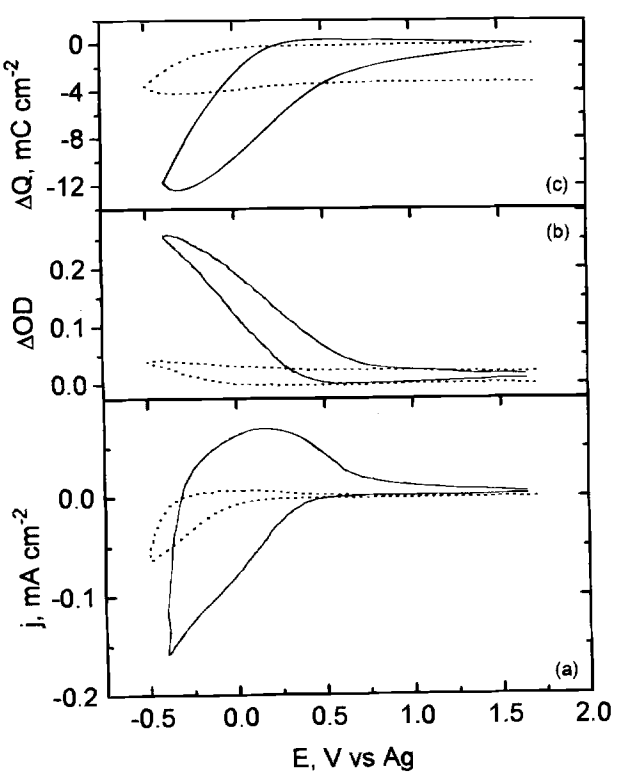

Fig. 5. Potentiodynamic experiment performed at 5 mV/s. Samples were MoO_x thin films deposited at ϕ = 1.65 sccm (solid curve) or σ = 8 sccm (dashed curve). (a) Current density *vs.* potential; (b) optical density change at λ = 632.8 nm *vs.* potential, and (c) charge change *vs.* potential.

Discussion

Figure 1 presents the behavior of the deposition rate with increasing oxygen flows in the sputtering chamber. According to reactive sputtering models,[9] the molybdenum oxide films deposited at low ϕ (region A, Fig. 1) come from the oxidation reaction occurring at the substrate surface. In region B (higher ϕ), the oxide films are formed from sputtering of molybdenum oxide generated at the target surface.[10] The initial increase in the deposition rate (region A, Fig. 1) is not clear, although it was observed elsewhere.[11] A lowering in the film density with an increase of the oxygen flow could explain these results. Also, a second explanation could be that at the beginning of the deposition process only metal atom's are being deposited. An initial increase in the oxygen flow causes an increase of the global sticking coefficient onto the substrate since the metal atoms sticking coefficient is nearly constant, and the oxygen atoms sticking coefficient increases with the increase of ϕ. The decrease in the deposition rate at region B (Fig. 1) is well studied. It is related to the oxidation kinetics tak-

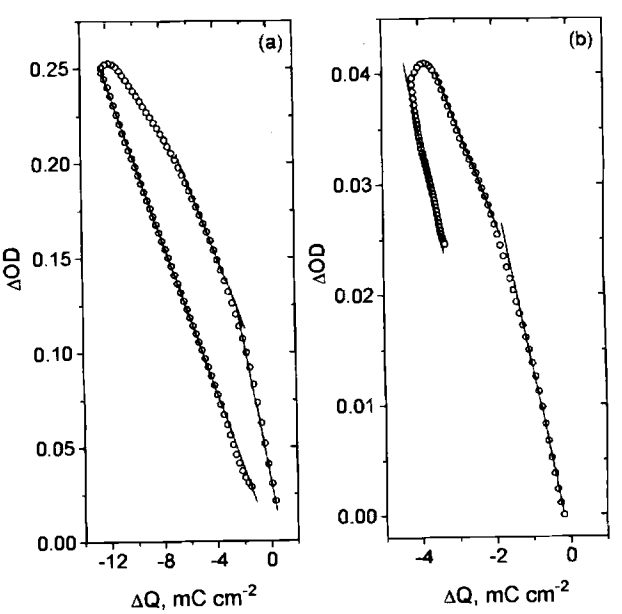

Fig. 6. Optical density change as a function of charge: (a) sample deposited at ϕ = 1.65 sccm and (b) sample deposited at ϕ = 8 sccm.

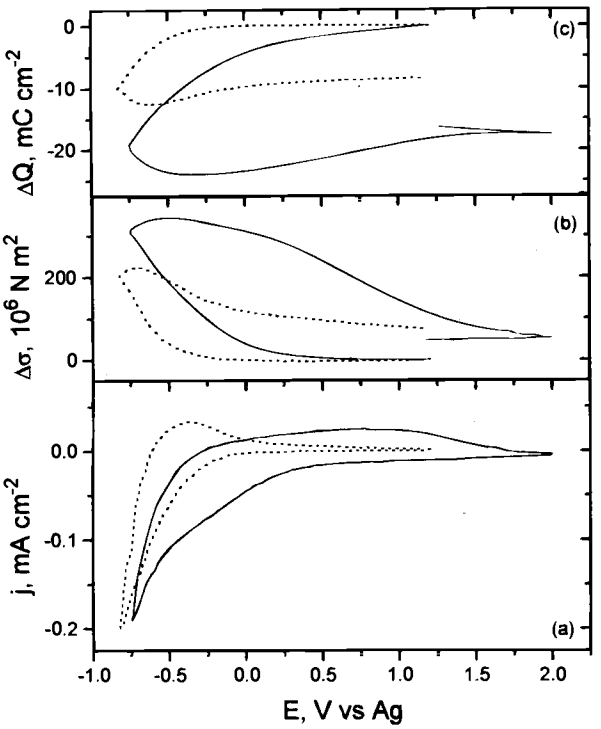

Fig. 7. Potentiodynamic experiment performed at 5 mV/s. Samples were MoO_x thin films deposited at ϕ = 1.75 sccm (solid curve) or ϕ = 8 sccm (dashed curve, same sample as in Fig. 5): (a) current density vs. potential; (b) stress change vs. potential; and (c) charge change as a function of potential.

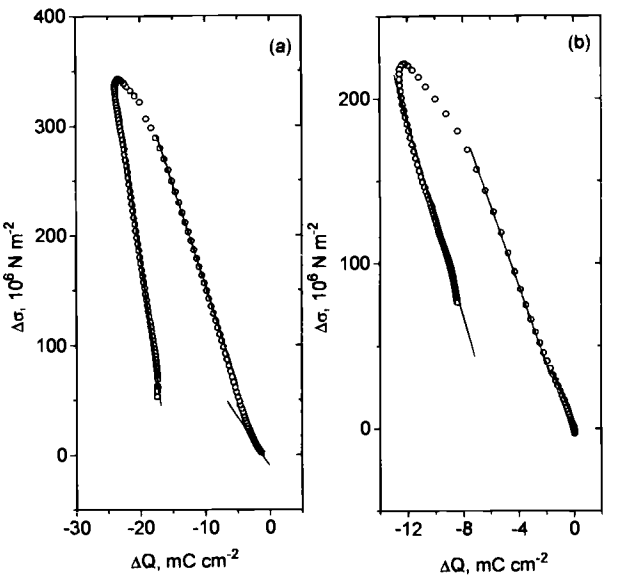

Fig. 8. Stress change as a function of charge; (a) sample deposited at ϕ = 1.75 sccm and (b) sample deposited at ϕ = 8 sccm.

ing place at the metal target[10, 12] and is mainly due to the low sputtering yield of the oxidized target.

Films deposited at ϕ = 1.5 sccm are composed of metallic Mo with oxygen in solid solution[13] and are not considered in this work. Values of the optical gap (Fig. 3) are in the range 2.8 eV for low ϕ to 3.2 eV at high ϕ, in good accordance with the values observed for amorphous molybdenum oxide films by Anwar and Hogarth.[2] Polycrystalline powder α-MoO_3 has an E_{opt} = 3.2 eV.[14] The polycrystalline α-MoO_3 film has an E_{opt} = 3.1 eV,[15] and the values for the β-MoO_3 forms are E_{opt} = 2.83 eV (powder)[14] and E_{opt}= 2.9 eV (film).[15] The blue color of films formed at low ϕ (Fig. 2), and the low values of their optical gap (Fig. 3) are clear evidence that they are substoichiometric molybdenum oxide, with composition MoO_{3-x} ($0 < x < 1$).[2,16] With the increase of ϕ, the oxygen vacancies (responsible for both substoichiometry and the blue color of the films deposited at low ϕ) tend to disappear, and the composition approaches that of the MoO_3 stoichiometry.

As has been shown in Fig. 4, the open-circuit potential varies by 0.3 V when the oxygen flow varies from ϕ = 1.65 to ϕ = 8 sccm. The B-films have the most positive potentials. As has been shown in Fig. 5 and 7, the range of electroactivity on potentiodynamic cycling is also displaced for the different films. We point out here that the observed span, both in the optical gap and in the open-circuit potential, are linked,[17] since both are dependent on the defective band structure of the material.

The following discussion addresses the behavior of the electrodes under potentiodynamic cycling. The j/E curves are smooth for both B- and T-films (Fig. 5a and 7a). This behavior is typical of amorphous films where no defined phase changes show up on intercalation.[6] The slow kinetics of the redox processes in these films could also be responsible for these smoothed curves.

For the B-films, lithium intercalation produces the highest optical density and stress changes (Fig. 5b and 7b). Smaller ΔOD and $\Delta\sigma$ values are systematically attained for the T-films. These results are in accordance with the higher charge capacity for the B-films, in comparison with the T-films. Substoichiometric amorphous molybdenum oxide films, in fact, contain oxygen ion vacancies that are positively charged structural defects. The higher charge capacity observed for the B-films is due to the higher concentration of oxygen vacancies for films deposited at low oxygen flows. From the optical viewpoint, B-films have a larger concentration of optically active centers than T-films do, since the electrochromism in substoichiometric molybdenum oxide films proceeds through an electric field assisted trapping of electrons at the positively charged defects.[18]

The coloration efficiency $\Delta OD/\Delta Q$ is a measure of the optical modulation per unit inserted or extracted charge. The higher values of $\Delta OD/\Delta Q$ observed for B-films indicate a higher absorbtivity for these films. It is hard to explain this behavior since the mechanism of optical absorption is not known for MoO_x films. For the most studied electrochromic material, WO_3, polaron absorption[1] conveniently describes the electrochromism. Also, intervalence charge-transfer and absorption by color centers have been pointed out as possible mechanisms.[1]

On the other hand, electrochromic materials are expected to obey the Lambert-Beer law. In this case, the coloration efficiency $\Delta OD/\Delta Q$ should be constant during the intercalation process. Our results showed that $\Delta OD/\Delta Q$ is not constant, being higher at the beginning of the cathodic process for both B- and T-films (Fig. 6). During the electrochemical reaction, both electrons and ions are inserted into the films. If charge neutrality exists during the reaction, the reaction rate should be governed by the smaller diffusion coefficient. Diffusion coefficients have been measured for MoO_x films. The lithium diffusion coefficient (D_{Li}) is in the range from 10^{-11} to 10^{-13} cm^2 s^{-1} (Ref. 1). Also, D_{Li} is concentration dependent. An electron diffusion rate in evaporated MoO_x films of $D_e = 8 \times 10^{-4}$ cm^2 s^{-1} was reported.[19] These results show that lithium diffusion into the films is rate determining. The accumulation of lithium ions near the film/electrolyte interface is the probable reason for the nonlinear behavior of $\Delta OD/\Delta Q$ in the cathodic cycle.

Stress variations, in the present experimental methodology, are a measure of the radius of curvature of the sample. Compressive stress (increase in $\Delta\sigma$) is associated with a global increase of the volume of the film. The fact that in the anodic cycle $\Delta\sigma/\Delta Q$ is lower for B-films than for T-films is an indication that the amorphous B-film has a

more open structure. The accumulation of lithium ions near the film/electrolyte interface, due to the low D_{Li} and its concentration dependence, can also explain the nonlinear behavior of $\Delta\sigma/\Delta Q$ in the cathodic cycle of the potentiodynamic experiments (Fig. 8). In the anodic cycle, stress changes show the relaxation of the system. In the experiments described in Fig. 7, the intercalated charge is higher for the B-films, in comparison with that for the T-films. Henceforth, the concentration of lithium ions near this interface is higher for the B-film, which could explain its higher $\Delta\sigma/\Delta Q$ in the anodic cycle.

Finally, it has to be pointed out that the dependence of the coloration capacity and the efficiency on the oxygen content of thin oxide films has been observed by other authors for MoO_x[3] and WO_x.[20] The *OD* change reported for B-films is greater than the value obtained by other authors, with similar films.[3]

Conclusions

In this work, we studied optical properties of as-grown and lithium-intercalated amorphous molybdenum oxide films. Stress changes during intercalation were also followed. We summarize below the main conclusions.

1. Films deposited at low oxygen flows (B-films) are substoichiometric molybdenum oxide with composition MoO_{3-x} ($0 < x < 1$). Films deposited at high oxygen flows (T-films) approach the MoO_3 stoichiometry.

2. B-films have a greater charge capacity, a greater concentration of optically active sites, and a more open structure when compared to T-films.

3. The coloration efficiency $\Delta OD/\Delta Q$ and the mechanical efficiency $\Delta\sigma/\Delta Q$ are not constant in the potentiodynamic experiments. A consequent conclusion is that the Lambert-Beer law is not valid for deep intercalation levels.

Manuscript submitted Dec. 11, 1995: revised manuscript received May 10, 1996.

FINEP Brazil assisted in meeting the publication costs of this article.

REFERENCES

1. C. G. Granqvist, *Handbook of Inorganic Electrochromic Materials*, p. 211, Elsevier Sci. Pub., Amsterdam (1995) (and references therein).
2. M. Anwar and C. A. Hogarth, *Phys. Status Solidi A*, **109,** 460 (1988).
3. N. Miyata and S. Akiyoshi, *J. Appl. Phys.*, **58,** 1651 (1985).
4. T. Maruyama and T. Kanagawa, *This Journal*, **142,** 1644 (1995).
5. A. Guerfi and L. H. Dao, *ibid.*, **136,** 2435 (1989).
6. C. Julien and G. A. Nazri, *Solid-State Batteries*, Kluver Academic Pub., Boston, Ma (1994).
7. J. Scarminio, S. N. Sahu, and F. Decker, *J. Phys. E., Sci. Instrum.*, **22,** 755 (1989).
8. J. Tauc, in *The Optical Properties of Solids*, F. Abeles, Editor, North Holland, Amsterdam (1972).
9. J. L. Vossen and W. Kern, *Thin Film Process*, p. 48, Academic Press, Inc., New York (1978).
10. A. F. Jankowski and L. R. Schrawyer, *Surf. Coat. Technol.*, **54/55,** 349 (1992).
11. D. A. Wruck, M. A. Dixon, M. Rubin, and S. N. Bogy, *J. Vac. Sci. Technol.*, **A9,** 2170 (1991).
12. T. Abe and T. Yamashina, *Thin Solid Films*, **30,** 19 (1975).
13. T. Yamaguchi and R. Miyagawa, *Jpn. J. Appl. Phys.*, **30,** 2069 (1991).
14. P. D. Fochs, *Proc. R. Soc. London B*, **69,** 70 (1956).
15. P. F. Garcia and E. McCarron, III, *Thin Solid Films*, **155,** 53 (1987).
16. V. K. Sabhapathi, O. Md. Hussain, P. S. Reddy, K. T. R. Reddy, S. Uthanna, B. S. Naidu, and P. J. Reddy, *Phys. Status Solidi A*, **148,** 167 (1995).
17. S. R. Morrison, *Electrochemistry at Semiconductor and Oxidized Metal Interfaces*, Plenum Press, New York (1980).
18. J. W. Rabalais, R. J. Colton, and A. Guzman, *Chem. Phys. Lett.*, **29,** 131 (1974).
19. O. Zelaya-Angel, C. Menezes, F. Sanchez-Sinencio, and G. L. Ferreira, *J. Appl. Phys.*, **51,** 6022 (1980).
20. S. Sun and P. H. Holloway, *J. Vac Sci. Technol.*, **A2,** 336 (1984).